Journal of Chromatography A, 1217 (2010) 7017–7023

Contents lists available at ScienceDirect

Journal of Chromatography A

journal homepage: www.elsevier.com/locate/chroma

Optimization of dispersive liquid–liquid microextraction and improvement of detection limit of methyl *tert*-butyl ether in water with the aid of chemometrics

Maryam Karimi[a], Hassan Sereshti[a,*], Soheila Samadi[a], Hadi Parastar[b]

[a] School of Chemistry, University College of Science, University of Tehran, P.O. Box 14155-64555, Tehran, Iran
[b] Department of Chemistry, Sharif University of Technology, Tehran, Iran

ARTICLE INFO

Article history:
Received 5 July 2010
Received in revised form 6 September 2010
Accepted 7 September 2010
Available online 21 September 2010

Keywords:
Dispersive liquid–liquid microextraction
Methyl *tert*-butyl ether
Gas chromatography–mass spectrometry
Chemometrics

ABSTRACT

Dispersive liquid–liquid microextraction (DLLME) coupled with gas chromatography–mass spectrometry-selective ion monitoring (GC–MS-SIM) was applied to the determination of methyl *tert*-butyl ether (MTBE) in water samples. The effect of main parameters affecting the extraction efficiency was studied simultaneously. From selected parameters, volume of extraction solvent, volume of dispersive solvent, and salt concentration were optimized by means of experimental design. The statistical parameters of the derived model were $R^2 = 0.9987$ and $F = 17.83$. The optimal conditions were 42.0 μL for extraction solvent, 0.30 mL for disperser solvent and 5% (w/v) for sodium chloride. The calibration linear range was 0.001–370 μg L^{-1}. The improved detection limit with the aid of chemometrics was 0.3 ng L^{-1}. The relative standard deviation (RSD) with $n = 9$ for 0.1 mg L^{-1} MTBE in water with and without internal standard was 2.7% and 3.1%, respectively. Under the optimal conditions, the relative recoveries of spiked MTBE in different water samples were in the range of 100–105%.

1. Introduction

Methyl *tert*-butyl ether (MTBE), a fuel additive produced from natural gas, has been used in gasoline at low levels since 1979 to replace tetra-ethyl lead in order to increase its octane rating as well as to help preventing engine knocking. However, it is currently used at much higher concentrations (up to 15 wt.%) as a fuel oxygenates to reduce the atmospheric emissions of carbon monoxide and hydrocarbons. MTBE is a volatile, flammable and colorless liquid which is relatively soluble in water and resistant to microbial decomposition and it is difficult to remove it in water treatment. It has also a rapid movement through soils and aquifers. MTBE's occurrence in the environment is of a great concern because of its toxicity and degradation products. MTBE often ends up in drinking water, negatively affecting its taste and odor, even at very low concentrations. The United States Environmental Protection Agency (US-EPA) has established a drinking water advisory for aesthetic concerns at 20–40 μg L^{-1} while the California State has recently set up a primary maximum contaminant level (MCL) of 13 μg L^{-1} for MTBE based on carcinogenicity studies in laboratory animals. Moreover, a secondary MCL of 5 μg L^{-1} was established in January 1999 for the taste and odor concerns [1,2].

The most common analytical methods that have been applied to the determination of MTBE include: direct aqueous injection (DAI) [3], static headspace (HS) analysis [4], purge and trap (PT) [5], solid-phase microextraction (SPME) [6] and Single drop microextraction (SDME) [7]. In DAI, sample pre-treatment and preconcentration have been eliminated, minimizing losses of volatile analytes as well as sample contamination. However, its main disadvantages are: (i) possible interferences due to matrix effects, and (ii) the non-compatibility of water with most capillary column stationary phases and with the widely used flame ionization detector (FID) [8]. Advantages of static headspace analysis are robustness, applicability to all sample matrices, and non-destructiveness to the samples that allows multiple analyses, but the reported detection limits are at least one order of magnitude higher than those for the other methods [9]. In PT, detection limits (typically in the ng L^{-1} to low μg L^{-1} range) are often more than 10 times lower than those achieved with static HS technique. Its main drawbacks, however, are: (i) the quite complex instrumentation that is required especially for on-line and real-time monitoring, (ii) possible water vapor interferences, (iii) cross contamination, and (iv) foaming. Besides, it is rather time-consuming which means that typical extraction times are in the 10–30 min range [8]. Solid-phase microextraction (SPME), a solvent-free sample preparation technique [10] integrates sampling, extraction, and concentration into a single step. However, it is expensive, its fiber is fragile and has a limited lifetime and sample carry-over can be a problem [11]. SDME is based on the distribution of the analytes between an

* Corresponding author. Tel.: +98 2161113632; fax: +98 2166495291.
E-mail address: sereshti@khayam.ut.ac.ir (H. Sereshti).

0021-9673/$ – see front matter © 2010 Elsevier B.V. All rights reserved.
doi:10.1016/j.chroma.2010.09.015

aqueous solution and a microdrop of a water immiscible organic solvent at the tip of a microsyringe needle. Its main advantages include the large reduction of solvent use, and the integration of extraction, reconcentration and sample introduction in one step. However, drop instability and the low sensitivity of the method are its main drawbacks [12]. DLLME was developed by Assadi and coworkers [11]. This method is based on ternary component (sample aqueous solution, extraction solvent and disperser solvent) that is a high performance and powerful preconcentration method. Simplicity of operation, rapidity, low time and cost, high recovery and enrichment factor are its main advantages. This method has been used for the determination of polycyclic aromatic hydrocarbons, organophosphorous pesticides, chlorobenzenes, phthalate esters, chlorophenols, and metal ions in the water samples [11,13–20].

In this work, DLLME coupled with GC–MS-SIM has been applied for the determination of MTBE in the water samples. The effective parameters on the extraction procedure such as volume of extraction solvent, volume of disperser solvent and salt concentration were studied and optimized using experimental design. Under the optimized experimental conditions, the detection limit and the dynamic linear range were evaluated and improved using chemometrics.

2. Experimental

2.1. Instrumentation

A gas chromatograph–mass spectrometer (Agilent Technologies 6890 GC system coupled with a 5973 network mass selective detector (MSD)) with a split/splitless injector system was used in all measurements. The injection port fitted with a 0.4 mm i.d. injector liner (Agilent) was operated in splitless mode, with the split purge valve opened 30 s after injection. The injection port temperature was 200 °C. Carrier gas was pure helium (99.999%) with a flow rate of 1 mL min^{-1}. Chromatographic separation was accomplished with an HP-1MS capillary fused silica column (30 m length; 0.25 mm i.d.; 0.25 μm film thicknesses, methyl polysiloxane, Agilent Technologies). The oven temperature was held at 50 °C for 10 min. The mass spectrometer was set in time scheduled selective ion monitoring (SIM) mode by recording the current of the following ions: *m*/*z* 57, 73 and 88. Mass spectra were taken at 70 eV. Mass range was from 20 to 500 amu. The injections into GC–MS were carried out using a 1 μL micro-syringe model Hamilton 7001 (USA). The centrifuge instrument model Hermle Z 200 A (Wehingen-Germany) was used for centrifuging.

An enhanced ChemStation G1701 DA version D.00.01.27 was used for the data collection and conversion to ASCII format. Data analysis was performed on a Pentium-based HP-Compaq personal computer. All of the chemometrics programs were coded in MATLAB v. 7.4 (Mathworks) for windows by authors. The statistical data were obtained using "Design-Expert 7.1.3 Trial" (Stat-Ease Inc., Minneapolis).

2.2. Reagents and solutions

MTBE, chloroform, chlorobenzene, tetrachloroethylene, trichloroethylene, carbon disulfide, ethanol, methanol, tetrahydrofuran, n-hexane, sodium chloride and carbon tetrachloride with the purity higher than 99% were purchased from Merck Chemical Company (Darmstadt, Germany). Pure helium (99.999%) was obtained from Hiva Gas Company (Tehran, Iran).

Standard stock solution of MTBE (1000 mg L^{-1}) in methanol was prepared, stored at 4 °C, and used within 1 month. Working aqueous MTBE solutions were prepared just before using from the stock solution. n-Hexane (1 mg L^{-1}) in trichloroethylene was used as internal standard.

2.3. Dispersive liquid–liquid microextraction procedure

A 2.00 mL working standard solution (1 mg L^{-1}) was placed in a 10 mL screw cap glass test tube with conical bottom and 5% (w/v) solid sodium chloride was added to it. Then, 0.30 mL of a solution containing methanol (as disperser solvent), 42 μL trichloroethylene (as extraction solvent) and 1 mg L^{-1} of n-hexane (as internal standard) was injected rapidly into the sample solution using a 1.0 mL syringe and the mixture was gently shaken. A cloudy solution (water, methanol, and trichloroethylene) was formed in the test tube. The mixture was then centrifuged for 3 min at 4500 rpm. The dispersed fine particles of extraction phase were sedimented in the bottom of the test tube. 0.50 μL of the sedimented organic phase was removed using a 1 μL micro-syringe and injected into GC.

3. Results and discussion

3.1. Selection of extraction solvent

The extraction solvent has to satisfy the following requirements: higher density rather than water, convenient extraction of analyte, good chromatography behavior, and low solubility in water. The selection of a suitable extraction solvent is very important for DLLME. Considering these properties, several solvents such as chloroform, chlorobenzene, tetrachloroethylene, trichloroethylene, carbon disulfide, and carbon tetrachloride were compared in the extraction of MTBE.

3.2. Selection of disperser solvent

Disperser solvent should be miscible with both water and extraction solvent. Methanol, ethanol and tetrahydrofuran were tested as disperser solvent. The experiments were performed using 0.5 mL of disperser solvent containing 35 μL of the extraction solvent. Methanol, as disperser solvent, showed the maximum extraction efficiency. Different combinations of extraction solvents and methanol were compared in the extraction of MTBE. Trichloroethylene (as extraction solvent) with methanol (as disperser solvent), showed maximum extraction efficiency (Fig. 1).

3.3. Optimization of dispersive liquid–liquid microextraction

In the next step, a central composite design (CCD) was used to optimize the effective DLLME parameters [21]. By a CCD it is also possible to identify the detailed dependence of different factors on

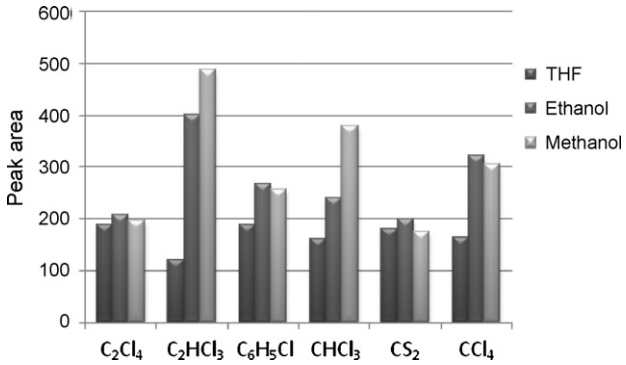

Fig. 1. Effect of different dispersive solvents with different extraction solvents on the efficiency of the extraction. *Extraction conditions*: sample volume, 2 mL; dispersive solvent, 0.50 mL; extraction solvent, 35 μL.

Table 1
Factors, their symbols and levels for central composite design.

Factor	Symbol	Levels				
		$-a$	−1	0	+1	$+a$
Volume of extraction solvent (μL)	E	15	22	32	42	49
Volume of dispersive solvent (mL)	D	0.16	0.30	0.50	0.70	0.84
Salt concentration (w/v %)	S	1.0	2.0	3.5	5.0	6.0

a response [22]. This design combines a two-level factorial design ($N_f = 2^f$) (f is number of factors) with additional star points ($N_a = 2f$), and the points at the center of the experimental region (N_0) which are usually repeated to get a good estimation of experimental error. Based on the preliminary studies and experiments, three parameters, volume of extraction solvent, volume of disperser solvent, and concentration of salt were studied. The star points are located at $+a$ and $-a$ from the center of the experimental domain [21]. The value of "a" needed to ensure orthogonality and rotatability can be calculated from Eq. (1) [23] and is equal to ±1.682. Then, N_0 was obtained equal to 9 using Eq. (2).

$$a = \sqrt[4]{N_f} \quad (1)$$

$$a = \sqrt{\frac{\sqrt{(N_f + N_a + N_0)N_f} - N_f}{2}} \quad (2)$$

Total number of experiments was calculated using Eq. (3) equal to 23.

$$N = 2^f + 2f + N_0 \quad (3)$$

In order to evaluate the work, the extraction recovery of MTBE was considered as the experimental response. The main factors, their symbols and levels, and CCD design matrix with responses are shown in Tables 1 and 2, respectively.

The software package, *Design-Expert 7.1.3* was used to analyze and plot the experimental data and related graphs. The analysis of variance (ANOVA) table was used to evaluate the model (Table 3). The *F*-value of 17.83 implies that the model is significant. The "lack of fit (*lof*) *F*-value" of 2.06 indicates its insignificance due to the error. Values of "Prob > *F*" less than 0.0500 indicate model terms are significant. In this case E and D are significant model terms. In this case, the second order polynomial with the most reasonable statistics, i.e. higher *F*- and *R*-values and low standard error was considered as the satisfactory response surface model for a central composite design to fit the experimental data. This model in terms of coded level factors is shown in Eq. (4); it consists of three main effects, three two-factor effects and three curvature effects:

Table 2
Design matrix and responses for central composite design.

Run	Block	E	D	S	Response[a]
1	1	22	0.30	5.0	36.01
2	1	32	0.50	3.5	49.33
3	1	42	0.30	5.0	80.42
4	1	22	0.30	2.0	46.90
5	1	42	0.70	2.0	46.59
6	1	32	0.50	3.5	45.19
7	1	22	0.70	5.0	30.53
8	1	22	0.70	2.0	25.89
9	1	32	0.50	3.5	52.84
10	1	42	0.70	5.0	52.47
11	1	42	0.30	2.0	68.12
12	1	32	0.50	6.0	56.30
13	1	32	0.16	3.5	63.49
14	1	32	0.50	1.0	51.37
15	1	15	0.50	3.5	20.68
16	1	49	0.50	3.5	76.31
17	1	32	0.84	3.5	41.28

[a] Extraction recovery.

$$Y = 49.31 + 14.72E - 8.30D + 1.48S - 2.87ED + 3.05ES + 1.14DS - 0.93E^2 + 0.41D^2 + 0.92S^2 \quad (4)$$

In Eq. (4), the positive and the negative coefficients of the main effects show that how the response changes regarding these variables. The absolute value of a coefficient shows the effectiveness of the related effect. For the graphical interpretation of the interactions, the use of three-dimensional (3D) plots of the model is highly recommended. The variables giving quadratic and interaction terms with the largest absolute coefficients in the fitted model were chosen for the axes of the response surface plots to account for curvature of the surfaces [24]. Therefore, the results were interpreted based on the graphs obtained from the model. Fig. 2 shows 3D plots of the model. The responses were mapped against two

Table 3
Analysis of variance (ANOVA) for central composite design.

Source	Sum of squares	d.f.[a]	Mean square	*F*-Value[b]	*p*-Valueprob > *F*[c]	Significance
Model	4137.42	9	459.71	17.83	0.0005	Significant
E	2985.81	1	2985.81	115.78	<0.0001	
D	940.33	1	940.33	36.46	0.0005	
S	29.80	1	29.80	1.16	0.3181	
ED	66.07	1	66.07	2.56	0.1535	
ES	74.60	1	74.60	2.89	0.1328	
DS	10.37	1	10.37	0.40	0.5461	
E^2	10.16	1	10.16	0.39	0.5501	
D^2	1.87	1	1.87	0.073	0.7954	
S^2	9.35	1	9.35	0.36	0.5661	
Residual	180.52	7	25.79			
LOF[d]	151.19	5	30.24	2.06	0.3580	Not significant
Pure error	29.33	2	14.66			

[a] Degrees of freedom.
[b] Test for comparing model variance with residual (error) variance.
[c] Probability of seeing the observed *F*-value if the null hypothesis is true.
[d] The variation of the data around the fitted model.

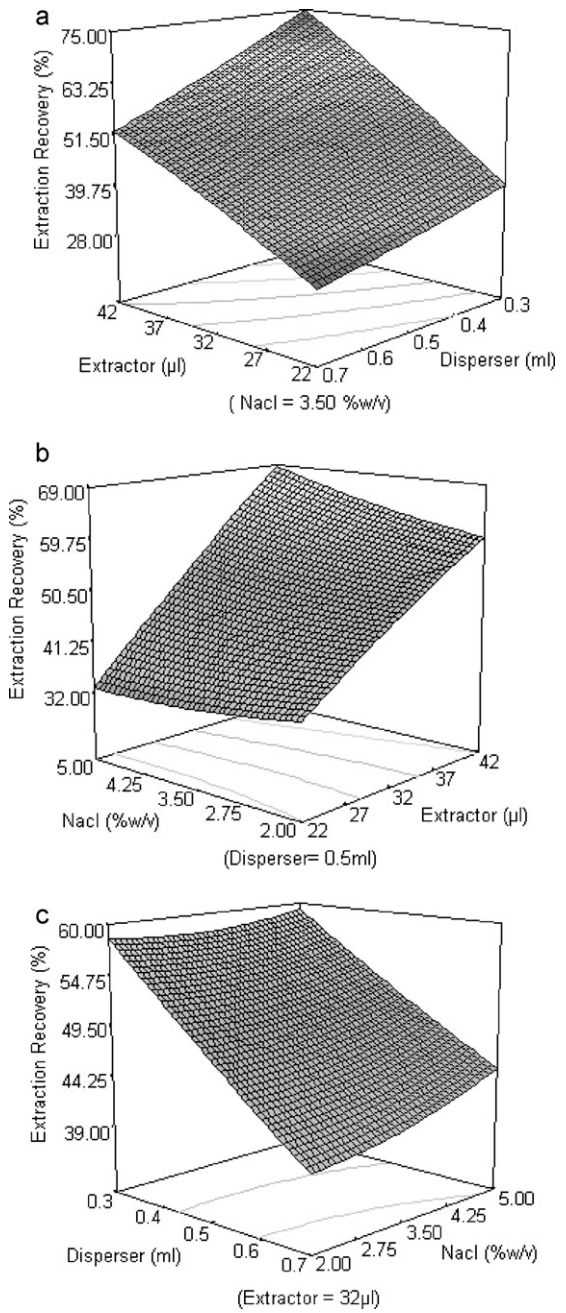

Fig. 2. Three-dimensional (3D) response surfaces for: (a) volume of extraction solvent–volume of disperser solvent; (b) volume of extraction solvent–concentration of salt; and (c) volume of disperser solvent–concentration of salt.

experimental factors while the third is held constant at its central level.

Fig. 2a and c shows that by increasing the volume of the disperser, the extraction recovery decreases, because the solubility of MTBE in water increases. On the other hand, from Fig. 2a and b it is obvious that the recovery increases by increasing the volume of extraction solvent. This is because the increased volume of organic phase causes more MTBE to be transferred from aqueous phase into it. Fig. 2b and c shows that the effect of concentration of sodium chloride on the extraction efficiency is not considerable. Finally, in order to obtain the optimal working conditions, we used optimization mode of the Design-Expert 7.1.3 software. The optimum value of parameters was 42 μL for extraction solvent volume (trichloroethylene), 0.30 mL for disperser solvent volume (methanol), and 5% (w/v) for sodium chloride.

3.4. Improvement of the detection limit using chemometric techniques

3.4.1. Theory

When a GC–MS measurement is performed, a two-way data matrix, **X**, can be obtained. In this data matrix, chromatographic time points define the row variables and m/z values define the column variables. The overall GC–MS signal can be divided into three constituting parts of analytical signal, background contribution and noise. Noise and baseline contribution are two fundamental problems in GC–MS analysis. Noise is generally defined as the instantaneously irreproducible signals caused by imperfections in the experimental apparatus and other regularities, by which the experimental results are often complicated. The effect of noise on analytical signals can be reduced using smoothing techniques. Among different techniques for smoothing, Savitzky-Golay filter [25] was used in this work. This filter uses a moving polynomial fit of any order, n, and the size of the filter consists of $(2n+1)$ points. Another serious problem in GC–MS analysis is that of varying baseline in combination with spectral background. This problem is a big one which generats loss of robustness and misinformation in an analytical method. Presence of baseline drift and/or spectral background can be detected using the appearance of GC–MS signal or the evolving latent projective graphs (ELPGs) [26]. Elimination of the chromatographic baseline has been shown to be a critical step for reducing the complexity of the sample matrix. With this aim, among the different strategies for baseline correction, we chose the methodology proposed by Liang and Kvalheim [26,27], the congruence analysis and least-square fitting.

Local analysis of the zero-component regions before elution of the first chemical component starts and after the last chemical component has eluted, can together provide sufficient information for correcting a drifting baseline. The procedure for confirming and correcting a systematically drifting baseline goes in five steps:

(1) Calculate the first normalized loading vector $\mathbf{p_{1,b}}$ for the zero-component region before (a) elution of the first chemical component starts and the first normalized loading vector $\mathbf{p_{1a}}$ for the zero-component region after (b) elution of the last chemical component is finished.
(2) Compare the two loading vectors by means of their congruence coefficient, i.e. calculate the scalar product $\mathbf{\Phi_{b,a} = p_{1,b}' p_{1,a}}$.
(3) If $\mathbf{\Phi_{b,a}}$ is close to 1.0 then $\mathbf{p_{1,a} = p_{1,b}}$ meaning that the baseline offset can be explained by the same factor (loading vector) during the whole chromatographic elution process. In this case, the "offset" vectors $\mathbf{t_b}$ and $\mathbf{t_a}$, are calculated for the two zero-component regions.
(4) Use the simple univariate least-square procedure to fit a straight line through all the elements of the "offset" vectors $\mathbf{t_b}$ and $\mathbf{t_a}$, with retention time as "independent" variable $\mathbf{t_i = b_0 + b_1 i}$, $\boldsymbol{i \in a}$, $\boldsymbol{i \in b}$. This procedure provides estimates of $\mathbf{t_e}$, for the baseline factor in the whole region between the two zero-component regions.
(5) Collect $\mathbf{t_b}$, $\mathbf{t_a}$, and $\mathbf{t_e}$, in one vector $\mathbf{t}$ and subtract $\mathbf{tl' + lp_{l,b}'}$ from the data matrix $\mathbf{X}$ to obtain a corrected chromatographic/spectroscopic data matrix.

It is concluded that correcting the background contribution from GC–MS signal and reducing its noise can improve the purity of signal and more analytical information can be obtained.

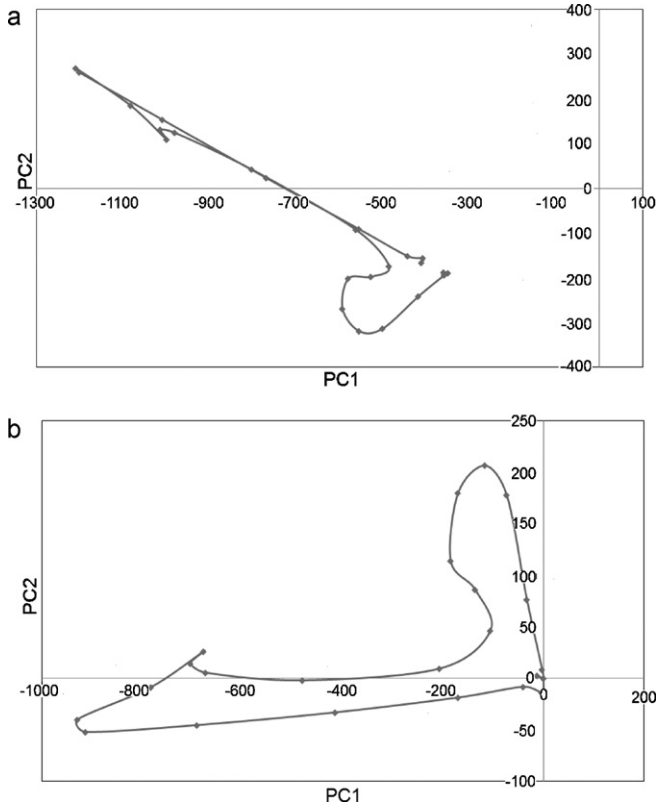

Fig. 3. ELPG graph: (a) before and (b) after baseline correction.

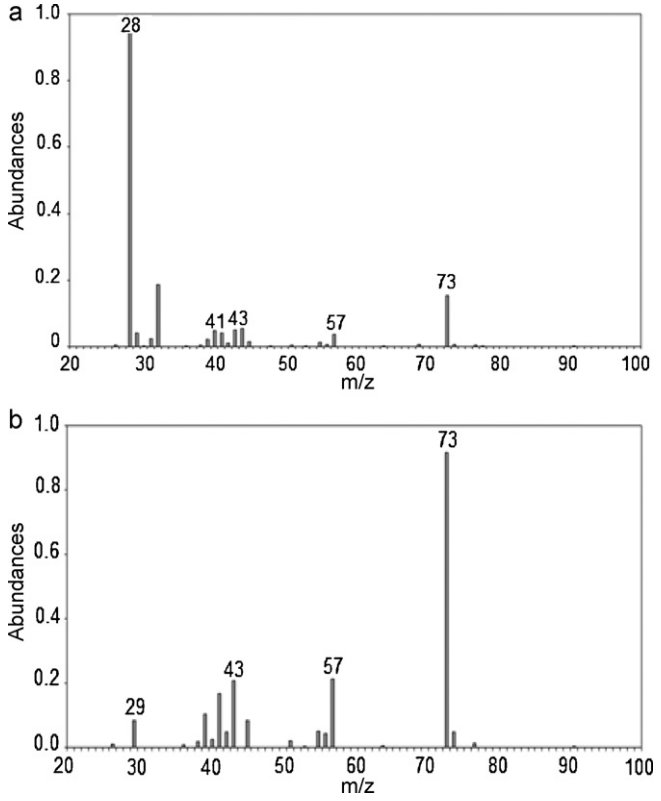

Fig. 4. Mass spectra of MTBE: (a) before and (b) after spectral background correction.

3.4.2. Chemometric analysis

For obtaining the LOD and linear dynamic range (LDR) for the proposed method the calibration curves were plotted in the proper concentration range from 0.5 ng L^{-1} to 370 μg L^{-1}. The peak area of MTBE in SIM mode was used as response. But in the concentration below 74 ng L^{-1} due to the presence of great amount of background in the MTBE peak, the peak area had near constant value. Therefore, the correlation coefficient of calibration curve is low in concentration range 1–74 ng L^{-1} (R^2 = 0.792). Using chemometrics, it is possible to correct background contribution, reduce the noise from target peak, and calculate the peak area. As mentioned before, congruence analysis and least-square fitting proposed by Liang and Kvalheim [26,27] and Savitzky-Golay filter [25] were used to correct background contribution and reduce noise, respectively and finally overall volume integration (OVI) [28,29] was used for peak area integration. In addition, the presence of background in data was confirmed using ELPGs. The ELPG is actually a principal component of projective plot. However, the presence or absence of spectral background is not easily observed from the chromatogram direction. Indeed, baseline offset and spectral background is most readily detected from ELPGs. Baseline offset is revealed when the ELPG graph fails to start and end at origin (zero concentration of chemical components). Fig. 3a and b shows the ELPG graph before and after baseline correction. Fig. 3a shows the large shift away from the origin and it is influenced by chromatogram or spectral background. After baseline correction the result in Fig. 3b was obtained. The result shows background removed from data. Fig. 4 shows correcting the spectral background for 37 ng/L of MTBE in scan mode. As it can be seen from Fig. 4a, m/z = 28 is the base peak and the characteristic m/z values of MTBE (m/z = 43, 57 and 73) have low intensities. However, correcting the spectral background results the mass spectrum that the contribution of artifact is reduced and characteristic m/z values of MTBE are significant (Fig. 4b).

The analysis of different GC–MS-SIM peaks shows the same background in low concentration. Therefore, background correction was performed for all data. After that, for reducing the noise in data, Svitzky-Golay filter was used with window width equal to 9 and polynomial order equal to 2. Finally, the peak area was calculated after signal processing. The peak area integration at every m/z point for each component can be easily calculated. Its sum, which is called the overall volume integration (OVI), is directly proportional to the content of the corresponding component. The advantage of OVI method prior to the peak area integration and peak splitting is that all mass spectra absorbing points are taken into consideration.

Using the above-mentioned conditions, the peak areas were calculated in each concentration. Fig. 5a and b shows the calibration curves after chemometric analysis. Due to the wide concentration range, calibration curve showed in overall concentration range from 1 ng L^{-1} to 370 μg L^{-1} (Fig. 5a) and in the lower concentration range from 1 ng L^{-1} to 74 ng L^{-1} (Fig. 5b). The correlation coefficient (R^2 = 0.9987) gets better and the slope of calibration curve (calibration sensitivity) is higher. For showing the art of chemometrics, the calibration curves before chemometric analysis and corresponding equations and statistics are shown in Fig. 6a and b. The limit of detection, based on signal-to-noise (S/N) ratio of 3 for the proposed method after chemometric analysis was 0.3 ng L^{-1}. It is interesting to note that LOD before chemometric analysis was 11.1 ng L^{-1}. It is concluded that chemometric analysis had great effect on the improving the analytical figures of merit. The reason may be related to significant reduction of undesirable phenomena during GC–MS analysis such as baseline drift, spectral background and presence of different types of noise. These problems are so effective at low concentrations of target analytes and can affect significantly the analytical results.

Table 4
Comparison of DLLME-GCMS-SIM with other methods for determination of MTBE in water samples.

Method	Detection system	LOD[a] (μg L^{-1})	LDR[b] (μg L^{-1})	RSD (%)	Reference
DLLME	GC–MS-SIM[c]	0.0003	0.001–370	2.7	proposed method
HS-SDME	GC-FID	0.06	0.1–500	4.8	[2]
DAI	GC–MS-SIM	0.10	0.1–10,000	<6%	[3]
PT[d]	GC-FID	2.00	2–80	2.0	[4]
HSDE[e]	GC-FID	7.00	10–10,000	5.5	[7]
HS-SPME	GC-FID	0.45	5–500	6.3	[21]
HS-SPME	GC–MS-FS[f]	0.01	0.02–5	10	[30,31]
DLLME	GC-FID	0.10	0.2–25	<5.1	

[a] Limit of detection.
[b] Linear dynamic range.
[c] Selective ion monitoring.
[d] Purge and trap.
[e] Headspace single drop extraction.
[f] Full scan.

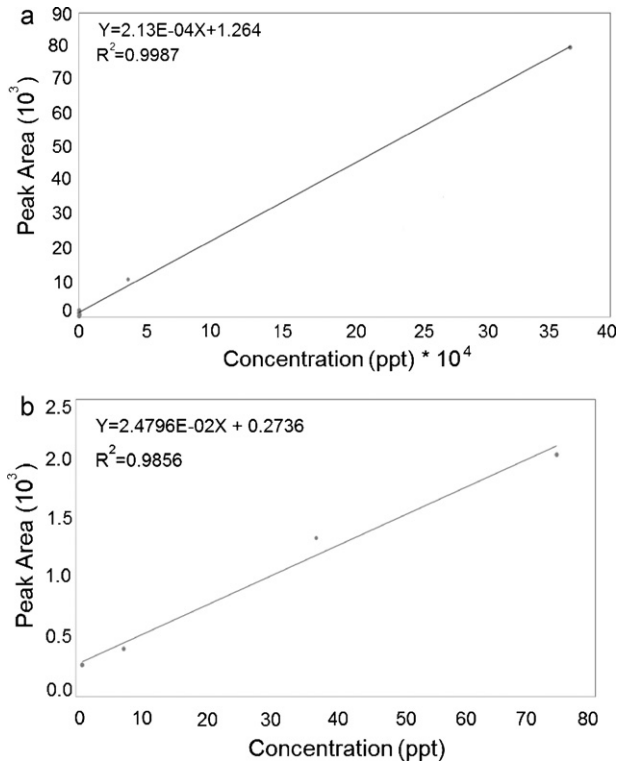

Fig. 5. Calibration curves after chemometric analysis: (a) 0.001–370 μg L^{-1}; (b) 0.001–74 μg L^{-1}.

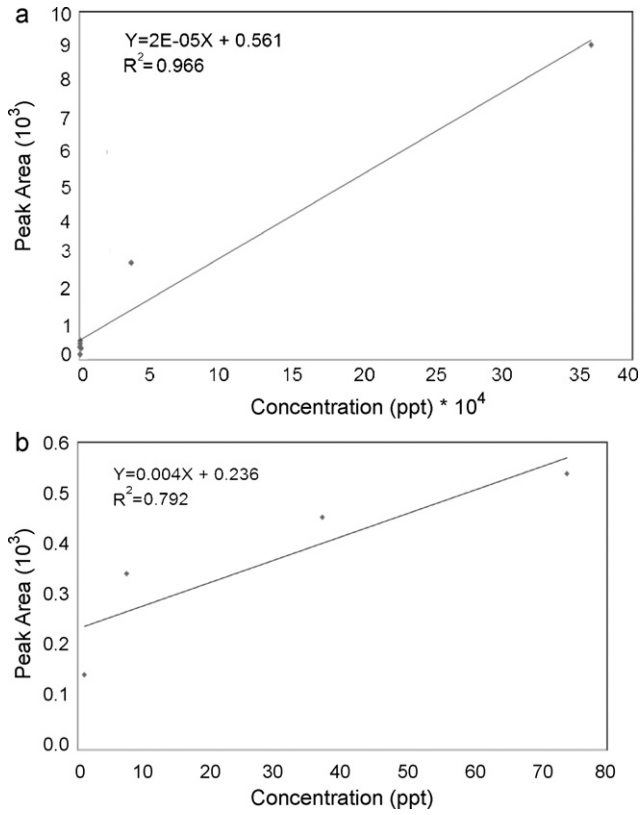

Fig. 6. Calibration curves before chemometric analysis: (a) 0.001–370 μg L^{-1}; (b) 0.001–74 μg L^{-1}.

3.5. Evaluation of the method performance

Under the optimal conditions, linearity of the method for the determination of MTBE in water samples was evaluated. The calibration curve was linear in the range of 0.001–370 μg L^{-1} with a correlation coefficient (R^2) of 0.9987. The limit of detection (LOD), based on signal-to-noise ratio (S/N) of 3 was 0.3 ng L^{-1}. The comparison of this method in terms of the figures of merit with other methods is shown in Table 4.

In order to examine analytical accuracy of the present method, relative recoveries of the spiked MTBE in different water samples

Table 5
Determination of MTBE in water samples at optimum microextraction conditions.

Sample	Concentration (μg L^{-1})	Added (μg L^{-1})	Found (μg L^{-1})[a]	Relative recovery (%)
Tap water[b]	n.f.[c]	60	63.2 (±2.5)	105
River water[d]	n.f.	60	61.3 (±2.2)	102
Well water[e]	n.f.	60	60.1 (±1.2)	100

[a] Mean ± SD, n = 3.
[b] Tap water was taken from university of Tehran.
[c] Not found.
[d] Sefid-rud river (Gilan province in the north of Iran).
[e] Well water was taken from a well in city of Tehran (capital of Iran).

(tap, river and well water) obtained by three replicate extractions at the optimal conditions (Table 5). It can be seen that the relative recoveries are in the range of 100–105% with a mean value of 103%. The relative standard deviation (RSD) with nine replicates at the center point of the parameters for a solution of 0.1 mg L^{-1} MTBE in water with and without internal standard was 2.7% and 3.1%, respectively.

4. Conclusion

In the present study, DLLME coupled with GC–MS-SIM was applied for the determination of MTBE in tap, river, and well waters. To find the optimal conditions of microextraction, and to improve the linear dynamic range (LDR) and limit of detection (LOD), chemometric techniques were applied. Experimental design was used to find the optimal conditions. Congruence analysis, Savitzky-Golay filter, and overall volume integration (OVI) were used for background correction, reducing the noise, and peak area integration, respectively. The correlation coefficient ($R^2 = 0.9987$) gets better and the calibration sensitivity is higher. The limit of detection, based on signal-to-noise (S/N) ratio of 3 before and after chemometric analysis was 11.1 ng L^{-1} and 0.3 ng L^{-1}, respectively. Therefore, chemometric analysis had a great effect on improving the analytical figures of merit. The comparison of the results obtained by the present work and other methods such as DAI, SPME, and PT showed it is fast and has a considerably low LOD and a relatively wide LDR.

References

[1] J. Arana, A.P. Alonso, J.M.D. Rodriguez, J.A.H. Melian, O.G. Diaz, J.P. Pena, Appl. Catal. B 78 (2008) 355.
[2] N. Bahramifar, Y. Yamini, S. Shariati-Feizabadi, M. Shamsipur, J. Chromatogr. A 1042 (2004) 211.
[3] C.D. Church, L.M. Isabelle, J.F. Pankow, D.L. Rose, P.G. Tratnyek, Environ. Sci. Technol. 31 (1997) 3723.
[4] B. Nouri, B. Fouillet, G. Toussaint, R. Chambon, P. Chambon, J. Chromatogr. A 726 (1996) 153.
[5] A. Tanabe, Y. Tsuchida, T. Ibaraki, K. Kawata, A. Yasuhara, T. Shibamoto, J. Chromatogr. A 1066 (2005) 159.
[6] F. Fang, C.S. Hong, S.G. Chu, W.P. Kou, A. Bucciferro, J. Chromatogr. A 1021 (2003) 157.
[7] A.S. Yazdi, H. Assadi, Chromatographia 60 (2004) 699.
[8] K. Demeestere, J. Dewulf, B. De Witte, H. Van Langenhove, J. Chromatogr. A 1153 (2007) 130.
[9] T.C. Schmidt, Trac-Trends Anal. Chem. 22 (2003) 776.
[10] C.L. Arthur, J. Pawliszyn, Anal. Chem. 62 (1990) 2145.
[11] M. Rezaee, Y. Assadi, M.R.M. Hosseinia, E. Aghaee, F. Ahmadi, S. Berijani, J. Chromatogr. A 1116 (2006) 1.
[12] J.L.P. Pavon, S.H. Martin, C.G. Pinto, B.M. Cordero, Anal. Chim. Acta 629 (2008) 6.
[13] S. Berijani, Y. Assadi, M. Anbia, M.R.M. Hosseini, E. Aghaee, J. Chromatogr. A 1123 (2006) 1.
[14] R.R. Kozani, Y. Assadi, F. Shemirani, M.R.M. Hosseini, M.R. Jamali, Talanta 72 (2007) 387.
[15] H. Farahani, P. Norouzi, R. Dinarvand, M.R. Ganjali, J. Chromatogr. A 1172 (2007) 105.
[16] N. Fattahi, S. Samadi, Y. Assadi, M.R.M. Hosseini, J. Chromatogr. A 1169 (2007) 63.
[17] E.Z. Jahromi, A. Bidari, Y. Assadi, M.R.M. Hosseini, M.R. Jamali, Anal. Chim. Acta 585 (2007) 305.
[18] A. Bidari, E.Z. Jahromi, Y. Assadi, M.R.M. Hosseini, Microchem. J. 87 (2007) 6.
[19] N. Shokoufi, F. Shemirani, Y. Assadi, Anal. Chim. Acta 597 (2007) 349.
[20] M.T. Naseri, M.R.M. Hosseini, Y. Assadi, A. Kiani, Talanta 75 (2008) 56.
[21] J. Dron, R. Garcia, E. Millan, J. Chromatogr. A 963 (2002) 259.
[22] T.A. Kokya, K. Farhadi, J. Hazard. Mater. 169 (2009) 726.
[23] E. Morgan, Chemometrics: Experimental Design, John Wiley, London, 1991.
[24] H. Sereshti, M. Karimi, S. Samadi, J. Chromatogr. A 1216 (2009) 198.
[25] R.G. Brereton, Chemometrics: Data Analysis for the Laboratory and Chemical Plant, Wiley, New York, 2002.
[26] O.M. Kvalheim, Y.Z. Liang, Anal. Chem. 64 (1992) 936.
[27] Y.Z. Liang, O.M. Kvalheim, A. Rahmani, R.G. Brereton, Chemom. Intell. Lab. Syst. 18 (1993) 265.
[28] F. Gong, Y.Z. Liang, Q.S. Xu, F.T. Chau, J. Chromatogr. A 905 (2001) 193.
[29] F. Gong, Y.Z. Liang, H. Cui, F.T. Chau, B.T.P. Chan, J. Chromatogr. A 909 (2001) 237.
[30] C. Achten, A. Kolb, W. Puttmann, Fresenius Anal. Chem. 371 (2001) 519.
[31] K. Farhadi, R. Maleki, N.M. Nezhad, J. Chin. Chem. Soc. 56 (2009) 575.